Journal of Inorganic and Organometallic Polymers and Materials (2020) 30:4677–4690
https://doi.org/10.1007/s10904-020-01602-w

Dual Responsive (pH and Magnetic) Nanocomposites Based on Fe_3O_4@ Polyaniline/Itaconic Acid: Synthesis, Characterization and Removal of Toxic Hexavalent Chromium from Tannery Wastewater

E. Parthiban[1] · N. Kalaivasan[2] · S. Sudarsan[3]

Received: 29 March 2020 / Accepted: 20 May 2020 / Published online: 2 June 2020

Abstract
A type of polyaniline (PANI) and itaconic acid (IA) with Fe_3O_4@PANI/IA magnetic nanocomposite was prepared via in-situ polymerization method. The Cr(VI) removal potential was examined in this work. Langmuir adsorption isotherm and Freundlich adsorption isotherm experiments was done in batch methods. Some parameters such as pH effect, dosage, contact time, and concentration of solutions were investigated in batch experiments. Structure and morphology of the nanocomposite were well characterized by FT-IR spectra, SEM, TEM, TGA/DTA, VSM, EDS and XRD studies. The results shows that the percentage of Cr(VI) removal (92.2%) has enhanced in PANI with IA nanocomposite. Considering all these results that the Fe_3O_4@PANI/IA nanocomposites have a promising adsorbent material for the removal of Cr(VI) ion from tannery wastewater.

✉ N. Kalaivasan
nkkvasan78@gmail.com

E. Parthiban
parthibantpgit@gmail.com

S. Sudarsan
srsudarsan29@gmail.com

[1] Department of Chemistry, Anna University, Chennai, Tamilnadu 600025, India

[2] Department of Chemistry, Thanthai Periyar Government Institute of Technology, Vellore, Tamilnadu 632002, India

[3] Department of Chemistry, C. Abdul Hakeem College of Engineering and Technology, Melvisharam, Tamilnadu 632509, India

Graphic Abstract

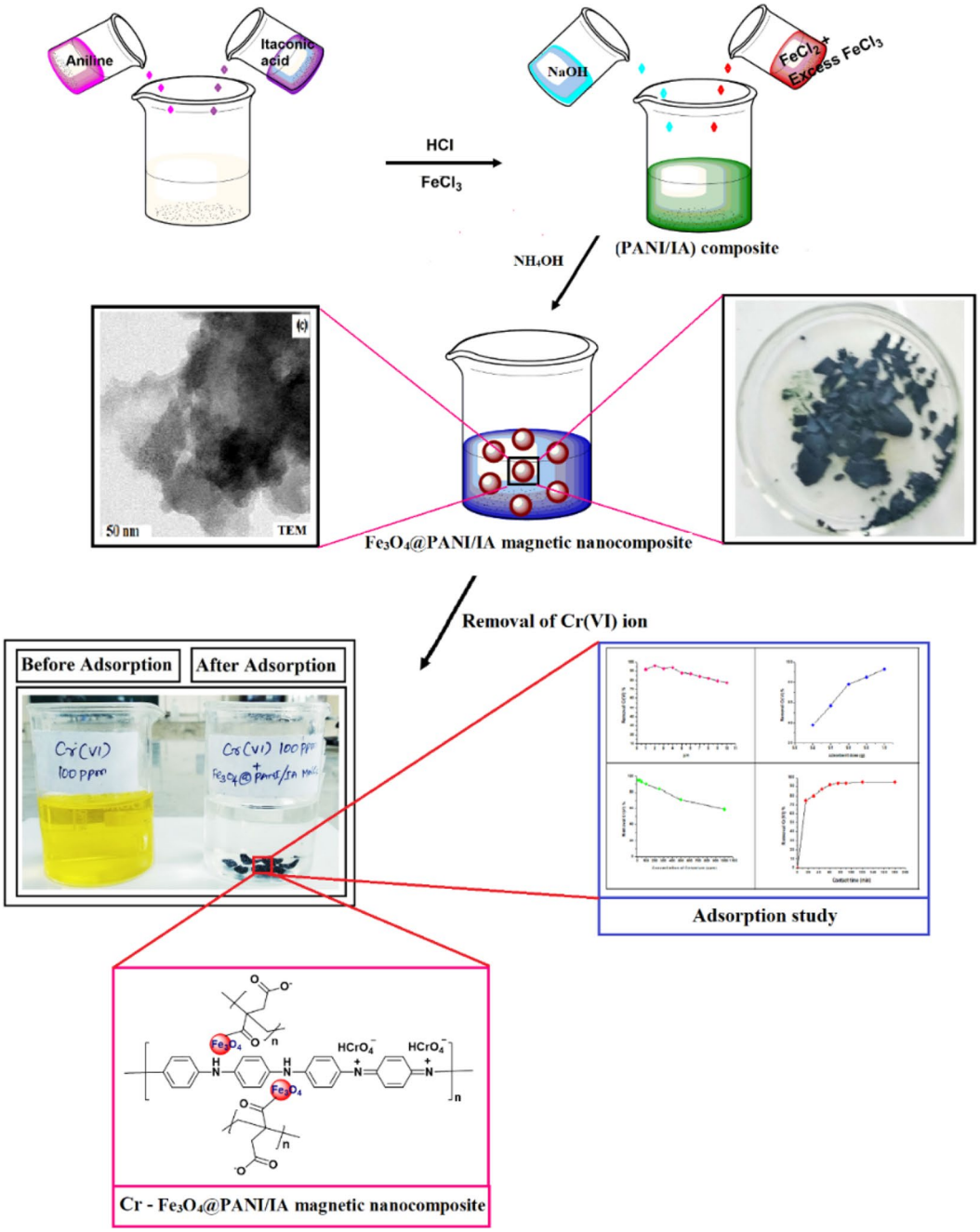

Keywords Itaconic acid · Nanocomposite · Adsorption · Wastewater · Chromium ion

1 Introduction

Heavy metal and toxic element contamination are an emergent issue affecting all living organisms throughout the world. The elimination of non-biodegradable toxic metals such as cadmium (Cd^{2+}), chromium (Cr^{6+}), mercury (Hg^{2+}), cobalt (Co^{2+}), lead (Pb^{2+}), ions using metal plating, tannery, mining, dyeing, printing, pigment, lead smelters, and chemical manufacturing industries causes for environmental and water pollution [1]. In general, Chromium exists in the environment as two forms viz, trivalent and hexavalent forms. The chromium (III) is most important to nutrition

conserving glucose levels and risk genotoxicity leads to cancer in human and living organisms. Nature of Chromium (VI) is chronic disorders, mutagenic, teratogenic and toxic against animals and human beings [2]. There are different treatment methods as already available to eliminate the toxic chromium ion such as crystallization, ultrafiltration, reverse osmosis, electro-dialysis, photocatalysis, ion exchange, adsorption, biosorption, and chemical precipitation [3].

Nowadays, nanotechnology produced different types of materials at the nanoscale level which have less than 100 nm [4]. Various multi-responsive magnetic nanocomposites a widely applicable in a numerable sector such as chemical engineering, manufacturing, detection of proteins biotechnology, biomagnetic separations, cosmetics, aquaculture technology, energy electronics, biopesticides, biosensors, anticorrosion, electromagnetic device applications and agriculture and plant sciences [5].

The conducting polymeric chain has shown different properties such as metallic, electronic, magnetic and optical properties which is due to π-conjugation. In 1976 a significant property has also been observed in polyacetylene [6]. The bifunctional polymer of polyaniline presence of the:NH_2 (amine) and NH^+ (imine) functional groups acting the excellent backbone used as chromium (III) and (VI) ions elimination of contaminated wastewater [7]. Polyaniline doped with sulfuric acid and Fe_3O_4@polyaniline/manganese dioxide composite using the removal of Cr(VI) metal ion [8, 9]. The PANI coated magnetite NCs and bacterial cellulose mat adsorbent material used exclusion Pb(II) and chromium ion real samples have been studied [10, 11].

Itaconic acid (IA) is a water-soluble white crystalline in nature. The presence of the unsaturated dicarboxylic multifunctional group in the IA has been helped to facilitate the hydrogen bonds with other side ionisable groups [12]. The soluble and conducting polyaniline–poly(itaconic acid) and gold nanoparticles anchored IA based nanocomposite have also been prepared by the chemical polymerization method [13, 14]. The dye adsorption of Poly(AA-*co*-IA) Hybrid nanocomposites are investigated by isotherm, thermodynamic and kinetic studies [15].

Various kinds of magnetic nanoparticles (MNPs) and their magnetic nanocomposites (MNCs) have been synthesized and used for high chemical stability, nontoxicity, and capacity. Many numbers of studies have been already carried out on MNCs such as; Protein digestion has also been mentioned PANI coated nano-Fe_3O_4/ CNTs composite [16], magnetic, conductive activities, and catalytic effect of iron oxide NPs and PANI/magnetite NCs [17], LPG and CO_2 sensing applications has also been dealed with nanorods of zinc ferrite thin films at room temperature [18], Polyaniline–Fe_3O_4 magnetic nanocomposite has been removed for acid violet 19 dye [19], magnetic properties and gas sensing applications of $Zn_xCu_{1-x}Fe_2O_4$ nanocomposites were also been examined via sol–gel method [20], multi-responsive applications of polyaniline@Almond shell bio composite [21], and reactive elimination of dye and magnetic separation properties were studied in superparamagnetic graphene based PANI/Fe_3O_4 and starch based MMT/PANI nanocomposite [22, 23]. Singh et al. also noticed the cobalt ferrite and ferric oxide for magnetic measurements and liquefied petroleum gas sensing behaviors applications [24].

These methods are an affordable and high cost for layer scale treatment for wastewater rich in Cr(VI). Adsorption using the PANI-IA-Fe_3O_4 magnetic nanocomposite is an efficient technique for the removal of the factory and industrial wastewater contamination of Cr(VI) and well fitted as compared to other techniques. The preparation method and commercial nanocomposite adsorbent are higher which makes the adsorption methodology costly. This kind of point indicates that the simple, convenient, and excellent adsorbent material of the chromium mixed industrial wastewater was desired for the present environmental and world problem.

In the present studies, as focused on the fabrication of Fe_3O_4@PANI/IA magnetic nanocomposite with different characterization. The type of magnetic nanocomposite is acted a competent adsorbent material for the chromium (VI) ion removal in industrial wastewater. The fabricated nanocomposite was characterized by different technique viz, FT-IR spectra, SEM, TEM, Energy-dispersive X-ray spectroscopy (EDS), thermogravimetric (TGA/DTA) and X-ray diffraction (XRD) analysis and VSM studies. The Fe_3O_4@PANI/IA magnetic nanocomposite has also performed by Langmuir adsorption and Freundlich adsorption isotherm. Several adsorption issues were examined the effect of pH, concentration, contact time, and dosage. The magnetic nanocomposite for adsorption isotherms dynamic to examine an involves of chromium removal from tannery wastewater.

2 Experimental

2.1 Chemicals

Aniline (ANI), Potassium dichromate ($K_2Cr_2O_7$) are obtained from Aldrich (India). Itaconic acid (Merck, India), Anhydrous $FeCl_3$ (SISCO, India), hydrochloric acid, ammonia (25% solution), sodium hydroxide, and Ethanol were purchased from Sigma Aldrich chemicals.

2.1.1 Heavy Metals

Potassium dichromate ($K_2Cr_2O_7$) 0.0023 mol was dissolved in 500 mL of distilled water to prepare stock solution 1000 mg L^{-1} of chromium (VI). The subsequent dilution stock solution through required concentrations was

prepared chromium (VI) solution used for all experiments 100 mg L^{-1}.

2.1.2 Sample of Industrial Wastewater

The wastewater collected from various tannery industries nearby Ranipet, Vellore district, Tamil Nadu, India. The wastewater contains toxic dyes viz., Azo dyes, methyl orange, methylene blue and light green which causes harmful effects to humans and the environment. The development of Fe_3O_4@PANI/IA MNCs followed by its Cr(VI) adsorption has been shown in **Scheme 1.**

2.2 Methods

2.2.1 Preparation of PANI

Initially, 0.03 mol of aniline (ANI) monomer was dissolved in 0.1 M hydrochloric acid solution in a beaker and 0.03 mol of anhydrous Iron(III) chloride were dissolved in distilled water and added dropwise to aniline solution was stirred for 5 h keep maintain temperature 0–5 °C. The product was filtered, washed more than a few times with distilled water ensue via ethanol and 24 h dried sample in the oven at 50 °C.

2.2.2 Preparation of Fe_3O_4@Polyaniline (PANI)/Itaconic Acid (IA) Magnetic Nanocomposite

To homogenize compounds were obtained and Itaconic acid (0.02 mol) was mixed to double distilled water (50 mL) with continuous stirring for 30 min and added aniline (ANI) monomer (0.02 mol) by the resulting solution was stirred for 1 h. In an ice bath, 0.04 mol of anhydrous Iron(III) chloride was put into the combination with uniform mechanical stirring overnight and mixture gradually sodium hydroxide solution at 10 °C. The washing product through double distilled water followed by ethanol and 24hrs dried nanocomposite in a vacuum oven at 50 °C. This magnetic nanocomposite was included in 50 mL of 0.5 M Ammonium hydroxide (NH_4 OH) for entire deprotonation and sample dried at room temperature 48 h used for characterization. Table 1 has been showed the feed composition of Fe_3O_4@PANI/IA nanocomposites.

3 Characterization

FT-IR spectrometer was measured by Alpha Bruker-2009 spectrum recorded over the wavelength region 400–4000 cm^{-1}. X-ray powder diffraction of polyaniline based magnetic nanocomposite measured using Bruker AXS D8 Advance powder diffractometer with Cu Kα radiation. Thermal stability was measured through the SDT Q600 model TG/DTA in the temperature range of 1200 °C. The UV–visible spectrophotometer was recorded on 200–800 nm by using (Double beam Shimadzu UV-2550) and pH meter adjusted at (pH 1–10) with appropriate buffer solutions. The morphology of Fe_3O_4@PANI/IA magnetic nanocomposite is observed using SEM (scanning electron microscope) the JSM-6701S at 0.3–30 kV and TEM and EDS analysis Model of FEI-TECNAI G2-20 TWIN with LaB6 filament at 200 kV. Magnetic properties of the Fe_3O_4@PANI/IA magnetic nanocomposite were measured using a VSM with Lake Shore 7404.

3.1 Adsorption Experiments

Magnetic nanocomposite Fe_3O_4@PANI/IA elimination of Cr(VI) from wastewater used as adsorption studies by batch experiment method. The different parameters such as 0.2–1.0 g (dosage), 10–1000 mL (volume), 1−10 (pH) and 15–180 min (contact time) have been studied. A $K_2Cr_2O_7$ (potassium dichromate) stock solution was taken in an Erlenmeyer flask [25]. The different concentration of chromium (VI) ion stock solution is prepared by the dilution method. A specific amount of magnetic nanocomposite (MNCs) added to 50 mL of concentration of chromium solution in water bath shaker for the time interval for all batch experiments are studied. The UV–Visible spectra characterized by remaining chromium (VI) and solution were making alkaline at pH ≥ 12 end of each adsorption experiment [26]. UV–Visible spectrophotometer is analysed potassium dichromate samples was prepared and each concentration of absorption is measured at λ_{max} 372 nm. The calculated using Eq. (1) of chromium (VI) removal percentage represented as

$$\% \text{ Removal} = \frac{(C_o - C_e)}{C_o} \times 100 \quad (1)$$

The following Eq. (2) was utilized to calculate the equilibrium sorption capacity.

Sorption capacity

$$q_e = \frac{(C_o - C_e)v}{m} \quad (2)$$

where, C_0 and C_e denote initial concentrations and a final concentration of Cr(VI) in (mg L^{-1}), q_e is the adsorption capacity of nanocomposite in (mg) of adsorbate chromium (VI) per grams of adsorbent Fe_3O_4@PANI/IA NCs. V is the volume of solution containing chromium (VI) (m^3) and m—weight of adsorbent NCs (Fe_3O_4@PANI/IA) (g).

3.2 Adsorption Isotherms

The isotherm of adsorption of Cr(VI) in the Fe_3O_4@PANI/IA MNCs has been investigated. Adsorption isotherm

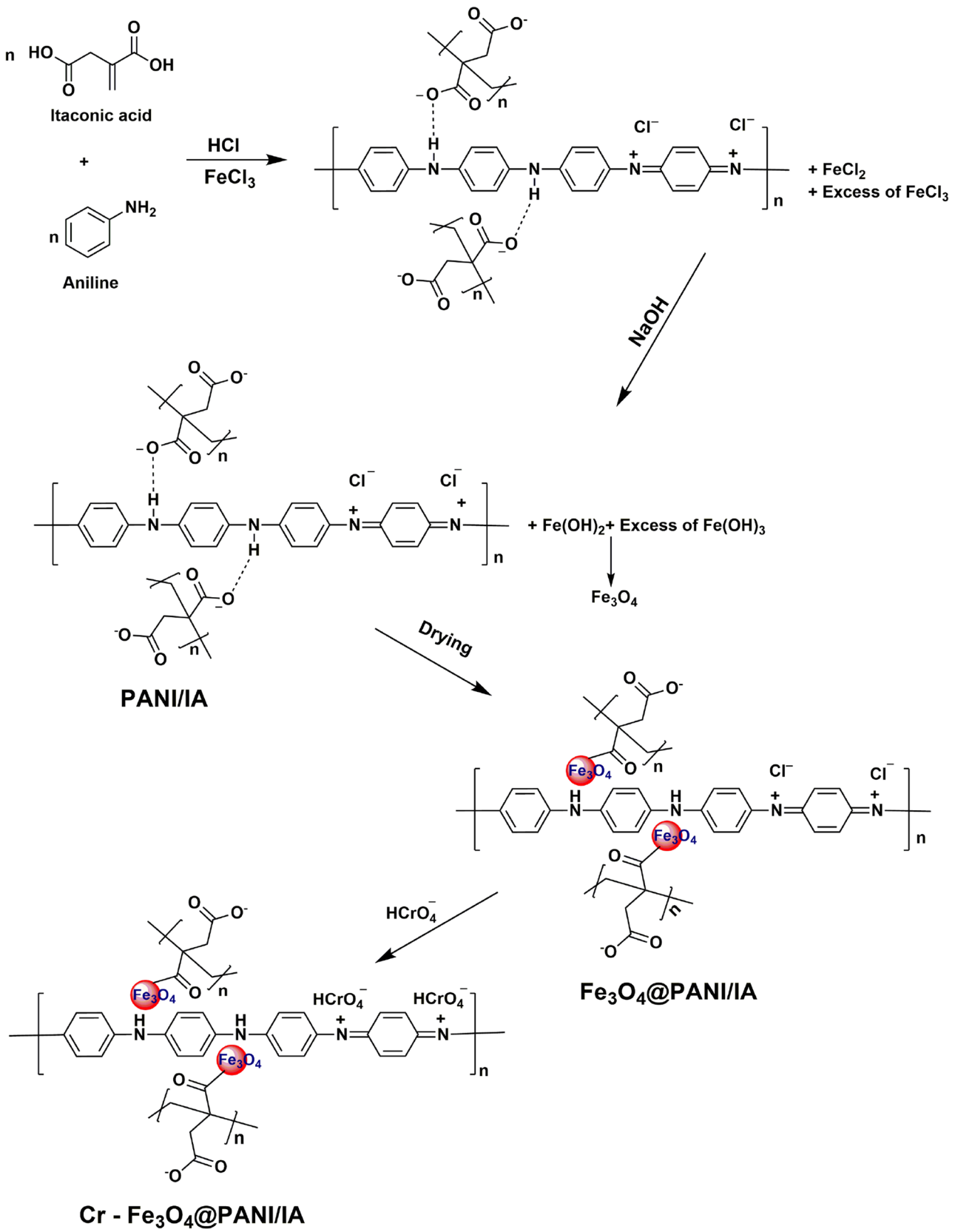

Scheme 1. shows the development of Fe3O4@PANI/IA magnetic nanocomposite followed by its Cr(VI) adsorption

Table 1 Stoichiometric quantities and physical exterior of Fe_3O_4@PANI/IA magnetic nanocomposites based on ANI, IA and $FeCl_3$ (unit: mol)

S. No	Sample code	Feed composition (mol)			Description
		ANI	IA	$FeCl_3$	
1	$A_1I_3F_4$	0.01	0.03	0.04	Dark blue, insoluble in water
2	$A_2I_2F_4$	0.02	0.02	0.04	Dark blue, insoluble in water
3	$A_3I_1F_4$	0.01	0.04	0.04	Dark blue, insoluble in water

models of Langmuir adsorption isotherm and Freundlich adsorption isotherm were explained by the interaction between adsorbed chromium (VI) and its concentration in solution under equilibrium condition.

3.2.1 Langmuir Adsorption Isotherm

In general, the linear form of Langmuir adsorption isotherm followed by Eqs. (3)

$$\frac{C_e}{q_e} = \frac{C_e}{Q_o} + \frac{1}{Q_o b} \tag{3}$$

where, C_e is the equilibrium concentration of metal ion (mg L^{-1}), q_e is the quantity of metal ion adsorbed per unit weight of sorbent (mg g^{-1}), Q_0 (mg g^{-1}) and b (L mg^{-1}) are Langmuir isotherm constants related to adsorption capacity [27].

3.2.2 Freundlich Adsorption Isotherm

The Eq. (4) is a linear form of Freundlich adsorption isotherm described a given below,

$$\log q_e = \log K_f + \frac{1}{n} \log C_e \tag{4}$$

where K_f and n Freundlich constants and indicates the favourably conditions for adsorption magnitude of the promoter 1/n lies between (0 and 1). The temperature increases with an increase in K_f values as an endothermic nature of the adsorption process [27].

3.2.3 Desorption and Regeneration Experiments

The adsorbents regeneration and reusable test conducted to desorption media for removal of chromium (VI) batch experiments. Adsorbent materials (1 g) added to 50 mL of chromium (VI) ions solution of the initial concentration of 300 mg L^{-1} for 3 h, at pH 2–4 with study of desorption and effluent of industrial heavy metal ion and organic dye

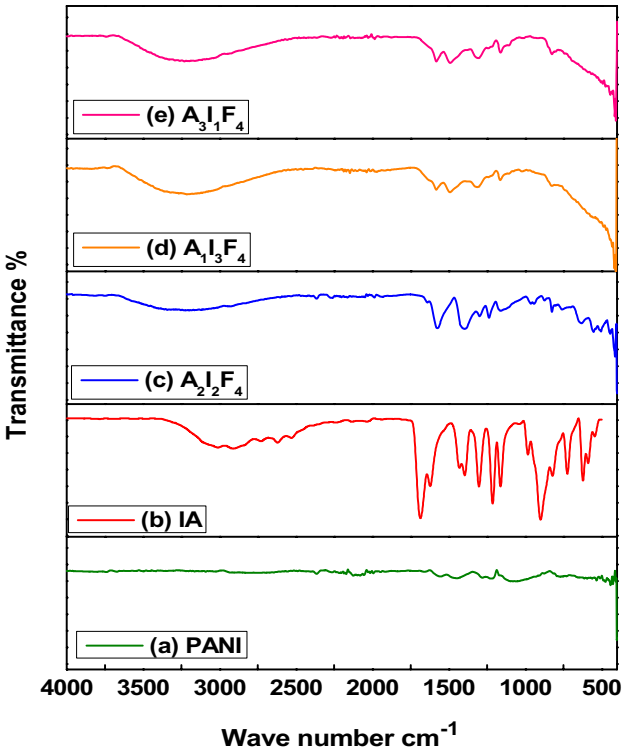

Fig. 1 FTIR spectra of **a** PANI, **b** IA, **c** $A_2I_2F_4$ **d** $A_1I_3F_4$ **e** $A_3I_1F_4$ magnetite nanocomposite

specific impurity was examined. After the adsorption process, desorption of metal ion from Fe_3O_4@PANI/IA was accomplished by treated nanocomposite (1 M HCl and 1 M NaOH) and after adsorbent washed with double distilled water. Correspondingly, to determine the reusability of Fe_3O_4@PANI/IA MNCs for elimination chromium (VI) used to adsorption and desorption process repeated in batch experiments.

4 Results and Discussion

4.1 FT-IR Spectra Analysis

Figure 1. has been shown the FTIR spectrum of (a) polyaniline (PANI), (b) itaconic acid (IA), a polymeric magnetic nanocomposite of (c) $A_2I_2F_4$, (d) $A_1I_3F_4$, (e) $A_3I_1F_4$. PANI absorption peaks at 1555 cm^{-1} and 1448 cm^{-1}, 1317 cm^{-1} and 1220 cm^{-1}, 1092 cm^{-1} and 852 cm^{-1} relates C=C stretching of quinonoid and benzenoid, C–N stretching vibration, C–H bending stretching vibrations of in-plane and out plane respectively (Fig. 1a) [28, 29]. The peak around 3010 cm^{-1} assigned to O–H stretching vibrations of IA and peak at 1686 cm^{-1}, 1430 cm^{-1} and 1210 cm^{-1} assigned to C=O, C–O–H in-plane and C–O the stretching vibrations (Fig. 1b).

The spectrum of $A_2I_2F_4$ magnetic nanocomposite showed a peak at 3160 cm^{-1} and 2633 cm^{-1} interaction between polyaniline and itaconic acid. The new peak observed at 1641 cm^{-1} and 1688 cm^{-1} attributed to $A_2I_2F_4$ magnetic nanocomposite formation which supports the disappearance of peaks (Fig. 1c) [13]. Itaconic acid doped polyaniline has shown the redshift broader shape undoped one sharp two peaks at 1305 cm^{-1} and 830 cm^{-1}. The absorption peaks at 1579 cm^{-1}, 1398 cm^{-1}, and 1163 cm^{-1} correspond to quinoid and benzene rings of C–N stretch vibration and a new peak has been absorbed in 1240 cm^{-1} itaconic acid doped polyaniline NCs [30]. The band at 580 cm^{-1} and 464 cm^{-1} observed to the pristine magnetite and new absorption peaks appear at 550 cm^{-1} and 447 cm^{-1} of Fe–O bond vibration in Fig. 1c. Shifting of the magnetite peaks has been displayed for the interaction of magnetite through polyaniline/itaconic acid [28]. Similar structural frequencies were also been observed in $A_1I_3F_4$ (Fig. 1d) and $A_3I_1F_4$ (Fig. 1e) magnetite nanocomposite supporting our mechanism of fabrication a unique structure of Fe_3O_4@PANI/IA magnetic nanocomposite.

4.2 X-Ray Diffraction Analysis (XRD)

The magnetic nanocomposite crystallinity has been investigated using the XRD spectra of polyaniline, Fe_3O_4@PANI/IA magnetic nanocomposite. The (Fig. 2a) characteristic peaks at 2θ of 15.4°, 20.7°, 25.2° and 35.7° corresponding to [011], [100], [110] and [200] crystal planes of polyaniline confirm that PANI is a retentive structure of crystalline [31]. Figure 2b has been shown the diffractogram of the synthesized Fe_3O_4@PANI/IA MNCs appear two peaks at 14.3° and 33.2° through a distance of 6.2 Å and 2.7 Å, respectively. Polyaniline–itaconic acid–matrix has been indicated the interaction between PANI and PANI-IA [13]. The Fe_3O_4@PANI/IA MNCs characteristic peaks appeared at 2θ of 15.2°, 21.4°, 32.9°, 42.8°, 53.9°, 57.1°, 64.3° and 84.2° corresponding to [111], [220], [311], [400], [422], [511], [440], and [642], respectively. The corresponding to magnetite (Fe_3O_4) has noticed as JCPDS number 19–0629 [32].

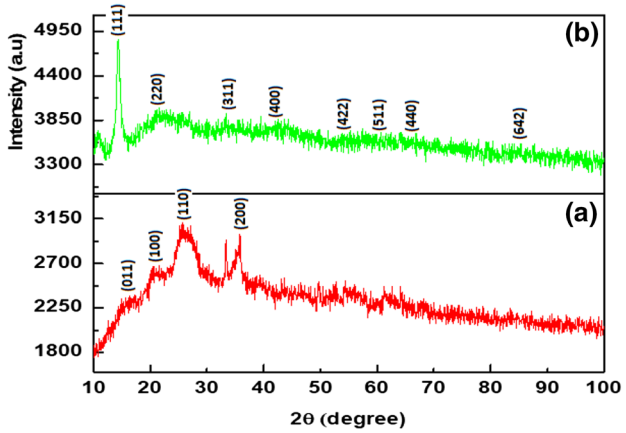

Fig. 2 XRD pattern of **a** PANI, **b** Fe_3O_4@PANI/IA magnetic nanocomposites

4.3 Thermal Analysis (TGA-DTA)

The TGA-DTA curves for Fe_3O_4@PANI/IA magnetic nanocomposite are presented in Fig. 3. The stage I decomposition of PANI occurs at 40 to 150 °C which is owing to the bounded water molecules is 21.9%. The stage II starting at around 150 to 545 °C almost 10.8% substance weight loss due to degradation backbone of itaconic acid and almost 28.2% weight loss for polyaniline nanocomposite decomposition at 780 °C in stage III. The nanocomposite total weight loss (61.0%) and iron oxide NPs (38.9%) and increase the thermal stability with addition of itaconic acid were used [22, 31, 33]. DTA curve for nanocomposite was observed an endothermic peak (320 to 390 °C) is removal of water molecule and exothermic peak (50 to 120 °C) is crosslinking of a polyaniline-itaconic acid polymeric matrix and sharp endothermic peak noticed at 700 to 720 °C (Fig. 3).

4.4 Magnetism (VSM) Analysis

VSM analysis used to examine the magnetic properties of Fe_3O_4@PANI/IA magnetic nanocomposite. Figure 4 has shown the magnetic hysteresis loop of Fe_3O_4@PANI/IA MNCs at room temperature that confirms the weak

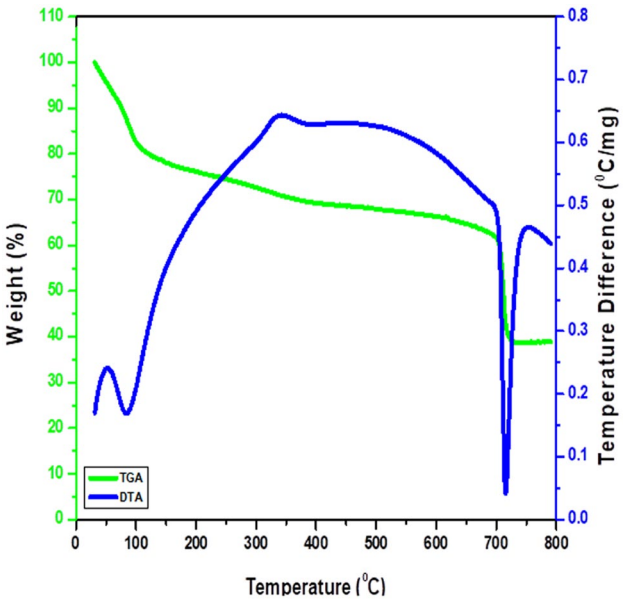

Fig. 3 TGA/DTA curves of Fe_3O_4@PANI/IA magnetic nanocomposite

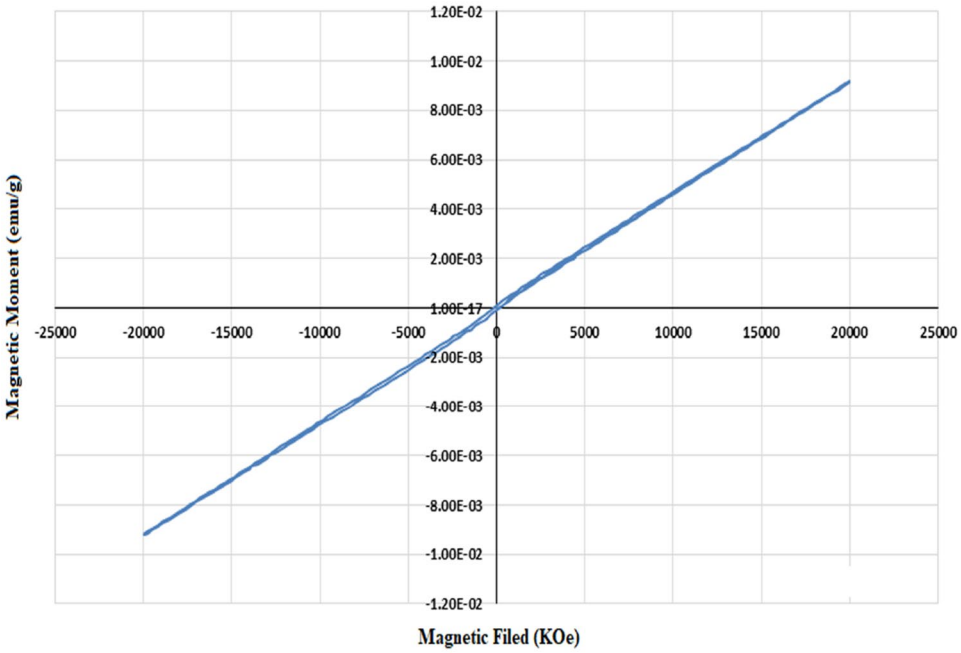

Fig. 4 Magnetization curves of Fe_3O_4@PANI/IA magnetic nanocomposite

paramagnetic properties of materials. The remanence or non-coercive force and linear relationship between applied filed and magnetization through positive (+ ve) slope of materials at room temperature and characteristic of the paramagnetic properties via saturation magnetization of Fe_3O_4@PANI/IA value were found to be 0.930 emu g^{-1} examined range of magnetic field (− 25,000 to + 25,000 KOe) in Fig. 4 [18, 34]. The surface morphology of Fe_3O_4@PANI/IA MNCs nanocomposite magnetization has been reduced due to the surface effect. PANI/IA based nanocomposite of a net magnetization has been reduced due to further reduction and well-known M–H curves performance character of nanocomposites matrix [20, 35].

4.5 SEM and TEM Morphologies

The SEM surface morphology of Fe_3O_4@PANI/IA magnetic nanocomposite has shown in Fig. 5a. This image has been revealing the prepared nanocomposite possess triangle and bar shape of nanostructures (Fe_3O_4) without aggregation on the polyaniline–itaconic acid matrix through a size of the particle about 5 µm [28, 33]. The above SEM image sizes have well supported the fabrication of nanoparticles within the polymeric matrix surface.

The TEM image of nanoparticles in Fe_3O_4@PANI/IA magnetic nanocomposite is presented in Fig. 5b–d. The Iron NPs found that various images of homogeneous distribution in Fig. 5b have shown the dispersion of Fe_3O_4 with polyaniline–itaconic acid matrix with low aggregation and typical images of HRTEM with high magnification resolution 50 nm at low aggregation (Fig. 5c). The bright circles which explain the crystalline structure of the iron nanoparticles by selected area electron diffraction (SAED) in (Fig. 5d). The obtained TEM images were revealed the formation of nanoparticles in the composites [28, 32].

4.6 EDS Analysis

The EDS spectra of Fe_3O_4@PANI/IA were used to measure and classify the elemental composition of the inclusion carbon (C), oxygen (O), and iron (Fe) (Fig. 5e). The nanocomposite clarified the distribution of iron NPs inside the PANI-IA matrix by SEM image. Figure 5e has been showed the nanocomposite percentage of iron 4.52%, 90.47% of carbon, 3.81% of oxygen, and 1.20% of copper. The intensity of the iron peak is proportional to the metal concentration of the iron nanocomposite has been confirmed by the iron nanoparticles in the conducting polymeric network.

4.7 Batch Experiments

The Chromium (VI) ion removal adsorption process was done by batch experiments and calibrated curves were plotted with various concentrations of Cr(VI) ion solution. To determine the optimum condition with various parameters were presented in Fig. 7.

4.8 Adsorption isotherms

Figure 6a, b have shown in the adsorption studies were using Freundlich and Langmuir adsorption isotherms plotted to the experimental data were studied. Freundlich

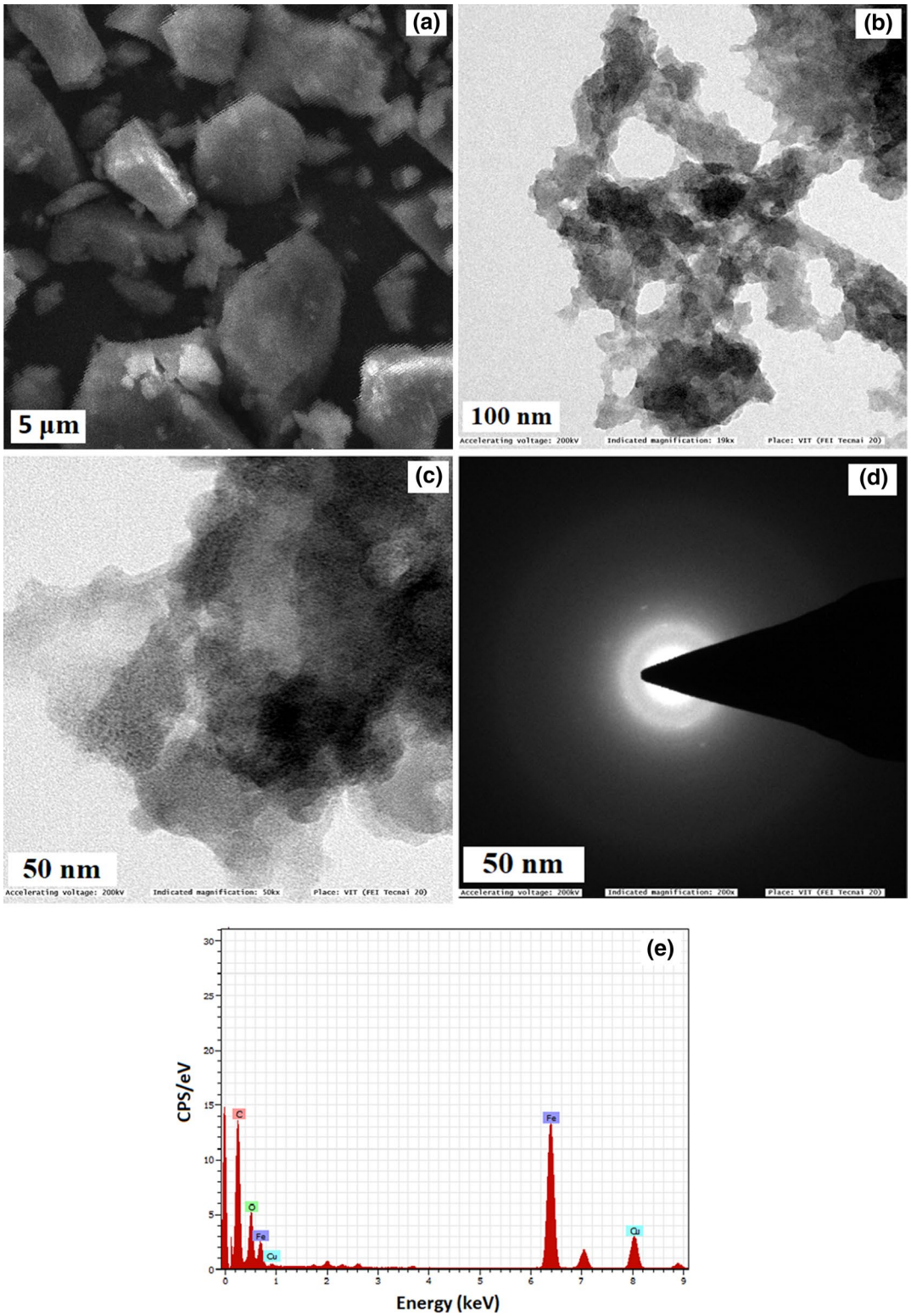

Fig. 5 **a** SEM image of Fe_3O_4@PANI/IA magnetic nanocomposite, **b** TEM image of Fe_3O_4@PANI/IA magnetic nanocomposite, **c** HRTEM image of Fe_3O_4@PANI/IA magnetic nanocomposite, **d** SAED of Fe_3O_4@PANI/IA magnetic nanocomposite, **e** EDS images of Fe_3O_4@PANI/IA magnetic nanocomposite

limits K_f (intercept) and n (slope) have mentioned as a value (n = 0.925) found after the graph are less than unity and signifying taking place of physisorption and graph plotted log q_e versus log C_e. Low n value proposes a low affinity among the Cr(VI)ion adsorbate and Fe_3O_4@PANI/IA MNCs adsorbent. Langmuir adsorption isotherm excellent results found that sorption studies proposed through the value of regression $R^2 = 0.968$ were studied and a graph plotted between 1/Ce versus 1/qe. The Cr(VI) removal of magnetic nanocomposite of Fe_3O_4@PANI/IA obtained maximum adsorption capacity (Q_0) is 218 mg g^{-1}. Table 2. has been shown on the Langmuir and Freundlich adsorption isotherms value. The type of adsorbent material has been mostly used for dye and toxic heavy metal ion removal applications [11]. The chromium (VI) ions removal using several adsorbents was described in given Table. 3. The Fe_3O_4@PANI/IA MNCs obtained adsorption capacity is significantly greater than other adsorbents. Moreover, it required cheap and less time duration to attain equilibrium of chromium (VI) removal MNCs and results are measured adsorbent used for chromium ion removal for industrial wastewater.

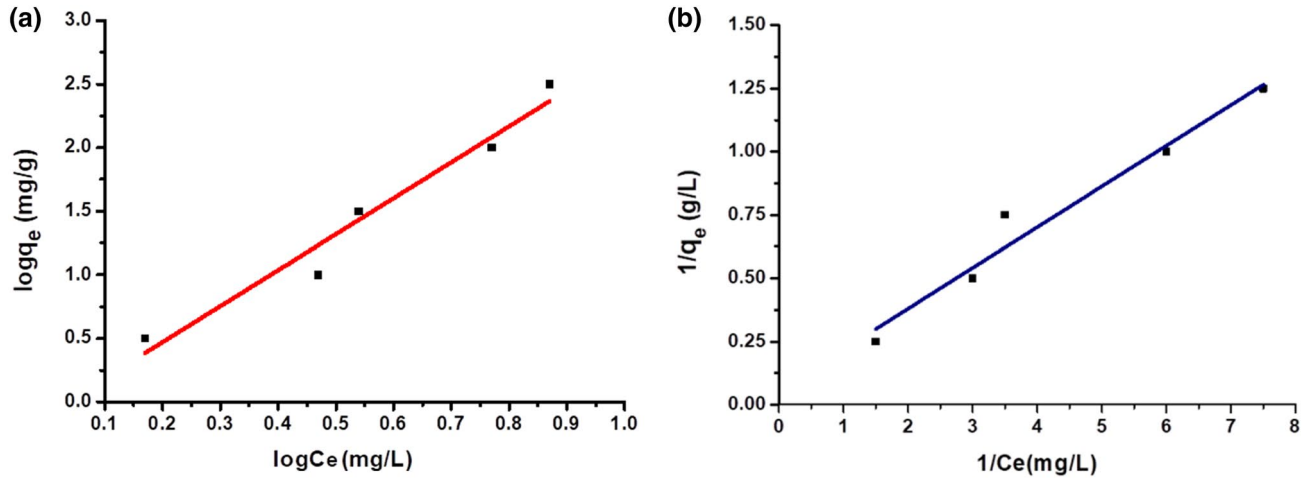

Fig. 6 **a** Freundlich adsorption isotherm of Cr(VI) by Fe_3O_4@PANI/IA magnetic nanocomposite, **b** Langmuir adsorption isotherm of Cr(VI) by Fe_3O_4@PANI/IA magnetic nanocomposite

Table 2 Freundlich and Langmuir adsorption isotherm parameters of Fe_3O_4@PANI/IA magnetic nanocomposite for the removal of Cr(VI) ions

Metal Ion	Adsorbent	Freundlich isotherm				Langmuir isotherm			
		K_F (mg/g)	1/n	n	R^2	q_m (mg/g)	b (L/mg)	K_L	R^2
Cr(VI)	Fe_3O_4@PANI/IA magnetic nanocomposite	86.21	0.0356	0.925	0.995	218	0.72	0.05	0.968

Table 3 Comparison of room temperature adsorption capacity and equilibrium time for the Fe_3O_4@PANI/IA magnetic nanocomposite with different adsorbents reported in the literature

Metal	Adsorbents	Adsorption capacity(mg/g)	Equilibrium time (min)	pH	Refs.
Cr (VI)	Polypyrrole/Fe_3O_4 magnetic nanocomposite	169.4–243.9	0.50–3	2.0	[35]
	PANI/humic acid composite	150	120	5.0	[36]
	PPY/ Fe_3O_4 microspheres	209	~ 70	2.0	[37]
	Fe_3O_4/PANI microspheres	200	180	2.0	[38]
	Flake-like PANI/montmorillonite NCs	168	150	2.0	[39]
	$NiFe_2O_4$–PANi nanocomposite	12.19	50	2.0	[40]
	Magnetite/graphene/polyaniline composite	153.54	40	2.0	[41]
	polyaniline-impregnated nanocellulose composite	92.59	60	6.0	[11]
	Fe_3O_4@Polyaniline/IA magnetic nanocomposite	218	60	2–4	*Present study

4.9 Adsorption Study

Chromium ion removal of the adsorption process using different parameters of pH, dosage, concentration, and contact time. The magnetic nanocomposite of Fe_3O_4@PANI/IA on the adsorption process is shown in Fig. 7.

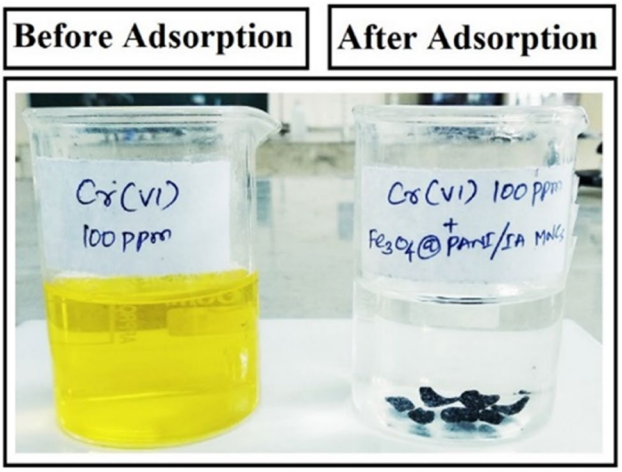

Fig. 7 Adsorption studies with Fe_3O_4@PANI/IA magnetic nanocomposite

4.9.1 Effect of pH

The consequence pH of chromium (VI) ion solution shows a vital character in the adsorption process. This surface charge and protonation functional groups on acted an adsorbent and adsorbate were absorbing chromium ions. Figure 8a has been displayed on the adsorption behavior of chromium (VI) in various pH of the solution has been studied from pH 2 to pH 10 by Fe_3O_4@PANI/IA magnetic nanocomposite. However, sorption study on the chromium (VI) by PANI based MNCs has been examined more 75–100 mg g^{-1} an acidic medium of pH 2–6 and alkaline medium of pH 8–10 and removal of dichromate ($Cr_2O_7^{2-}$) lesser pH levels of chromium (VI).

Adsorbent reaches a positive charge due to amine groups protonation of Fe_3O_4@PANI/IA magnetic nanocomposite. It removes dichromate ($Cr_2O_7^{2-}$) anions with electrostatic attraction. The Acidic pH of polyaniline presence in Fe_3O_4@PANI/IA magnetic nanocomposite attains its condensed naturally electrons transfer through chromium (VI) ions. The Comparable, trends have also been observed in PANI/PVA and Polyaniline/humic acid nanocomposite by removal of Cr(VI) sorption capacity high at acidic region and occurrence of oxygen and nitrogen atom adsorbed chromium (VI) reduced to low poisonous chromium (III) ions [42]. A competition occurred between the $Cr_2O_7^{2-}$ ions and OH^- ions on the sorption positions of the adsorbent surface found that lower at higher pH. The dissolution amphoteric solid occurred in the low and high pH 2–10 and iron oxide solubility of adsorbents aqueous solution value seeing. Among, the activity of magnetite mostly dissolves greater than iron (III)oxide due to iron (II) oxide. The dissolved iron (III) oxides leftovers less (11−4 mol dm^3) between pH (2–10) and so neglected in the pH range of adsorption on magnetite examined [43].

4.9.2 Effect of Adsorbent Dose

Figure 8b. has been shown on the different adsorbent dosage ranging (0.2–1.0 g) used to Fe_3O_4@PANI/IA magnetic nanocomposite and adsorption of chromium (VI) solution enhanced through the increase of MNCs dosage because available of adsorption sites is very high and removal percentage has been increased from 38 to 93% at a dose of 0.2–1.0 g. The adsorbent 1.0 g was initiate optimal dosage of chromium (VI) ions removal 93% [8]. Hence, more than 99% of removal chromium (VI) ion attained via synthetic Fe_3O_4@PANI/IA magnetic nanocomposite.

4.9.3 Effect of Contact Time

The increases with the increase retention time an adsorption is a removal of chromium (VI) in the magnetic nanocomposite have been carried out for the various time intervals of 15–180 min [8]. Removal percentage of chromium (VI) gradually increases with time 15–60 min. The effectively 60 min more than 92% were removed by the adsorption process thereafter it becomes increases gradually and also discussed by Jahan et al. (Fig. 8c) [11]. However, the range equilibrium in chromium (VI) sorption on polyaniline based humic acid and chitosan nanocomposite has been required at 120–240 min [42, 44]. This type of MNCs used to remove toxic metal ion from wastewater by quickly and its attained adsorption equilibrium much less retention time at 60 min. Further mixing of polyitaconic acid (PIA) is increasing sorption capacity left out altering the sorption model on polyaniline.

4.9.4 Effect of Concentration

The adsorption properties of different concentrations of Fe_3O_4@PANI/IA magnetic nanocomposite as a removal percentage of chromium metal ion like 10–1000 mg L^{-1} through an optimum (pH 2) and contact time (60 min) correspondingly (Fig. 8d). Addition of (1.0 g) dry adsorbent into (50 mL) chromium ions solution by the various concentrations. The results obtained as clearly explain at low concentration maximum adsorption takes place. The increases concentration and decreases chromium (VI)

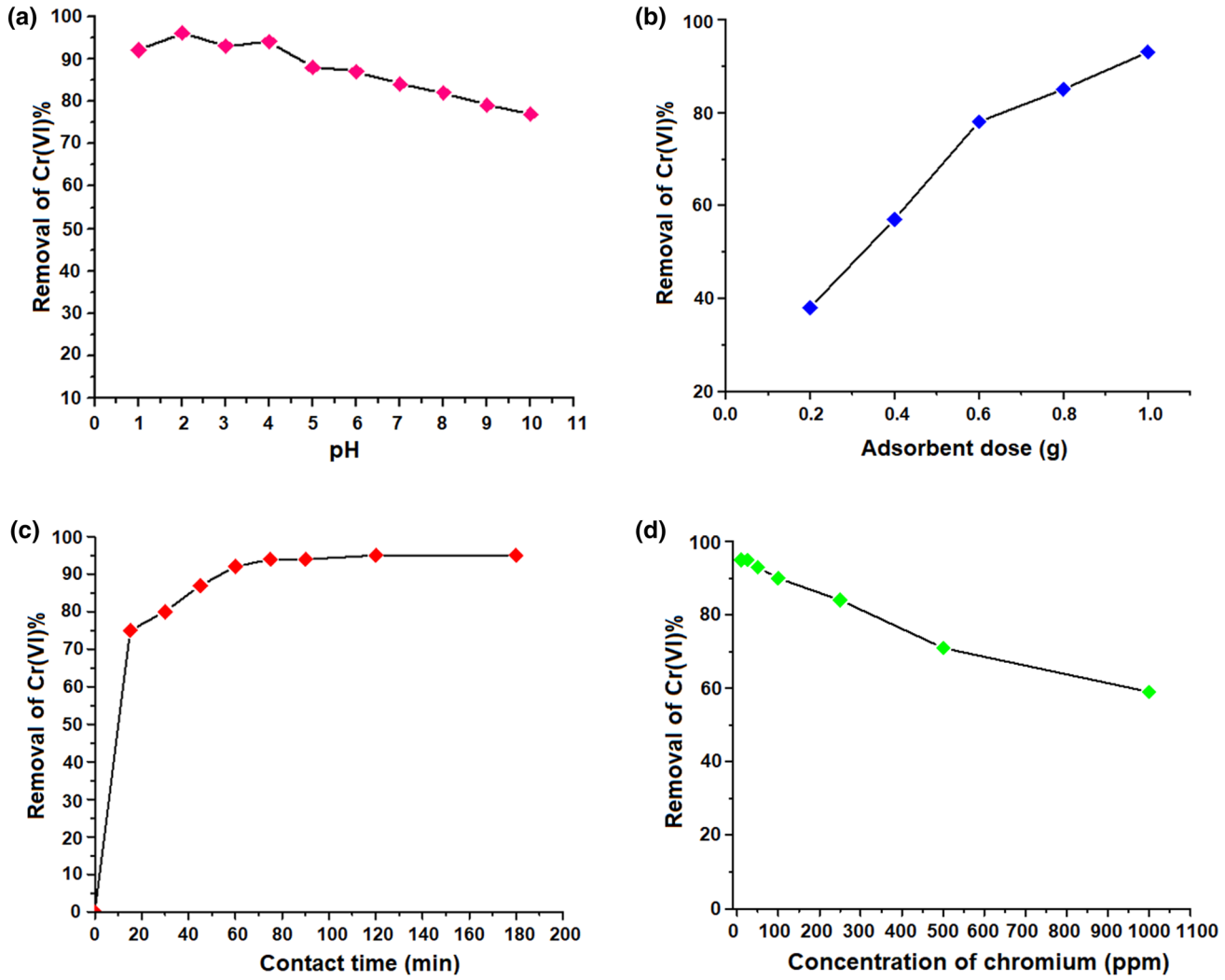

Fig. 8 **a** Effect of pH, **b** Adsorbent dose, **c** Contact time and **d** Chromium concentration on adsorption process of Cr (VI) by Fe_3O_4@PANI/IA magnetic nanocomposite

removal percentage due to the all vacant on cavities were filled to allow the saturation. The nanocomposite various concentrations from involved in maximum removal tendency Cr(VI) for 95% with 100 mg L^{-1} of optimal value [7, 45].

4.10 Industrial Wastewater Samples for Adsorption Experiment

Industrial wastewater was tested by synthesized Fe_3O_4@PANI/IA magnetic nanocomposite can be used an adsorbent for 3 h by batch adsorption experiments method. Figure 9 has been observed results percentage 92.2% of removal toxic heavy metal into Chromium (VI) ions. Table. 4 has been summarized results for MNCs using before and after wastewater treatment.

4.11 Mechanism Removal of Chromium (VI) from Wastewater

Hexavalent chromium removal from the wastewater mechanism was scrutinizing the determination of pH solution. The pH range of (8–10) improves adsorption (%) of Cr(VI) ions gradually. The maximum removal has shown at pH 10 above that pH yielded an a constant in adsorption case chromium ions, which appear at lower pH of Van der Waals forces attraction leads to form precipitation residue a toxic chromium ion and higher pH of magnetic nanocomposite (−ve) charged places attract (+ve) charged toxic metal cations by electrostatic interaction has greater compared to acidic pH. The dia functionalized polyaniline polymeric matrix has contributed an actual chromium ions removal from the aqueous system [11].

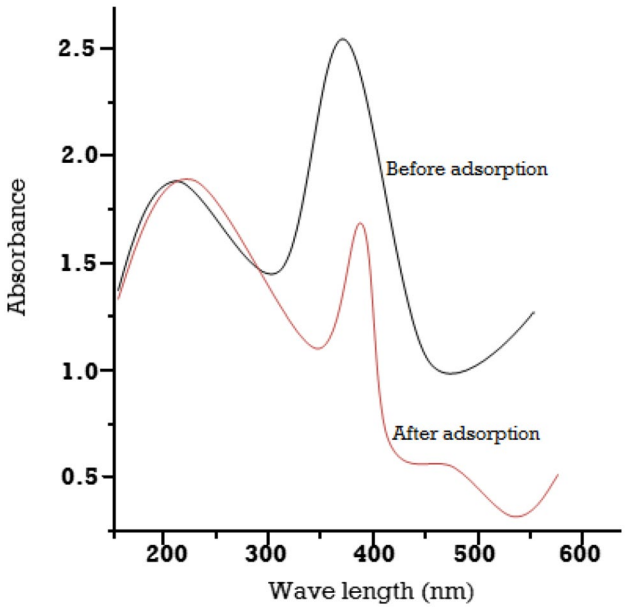

Fig. 9 Absorption spectrum for before and after treatment of industrial wastewater sample

Table 4 Before and after treatment of waste water samples using Fe_3O_4@PANI/IA magnetic nanocomposite

Constituents in waste water	Before treatment	After treatment
pH	8–10	6.5–7
Total dissolved solids (ppm)	3600	900
Total suspended solids (mg L^{-1})	450	< 72
Biological oxygen demand (mg L^{-1})	950	< 45
Chemical oxygen demand (mg L^{-1})	2000	< 150
Oil and grease (mg L^{-1})	41	< 15
Heavy metal: Cr (ppm)	100	< 1

4.12 Re-Usability Studies

In general, after the usage of adsorbent were throughout the environment which leads to taking pollutant. To concentration, the above issue, the recovery of adsorbent of Fe_3O_4@PANI/IA magnetic nanocomposite was done by regeneration studies (Fig. 10). The nanocomposite observed various concentrations through desorption reagents like an acidic, basic and neutral medium. Fe_3O_4@PANI/IA magnetic nanocomposite (0.05 g) was filled by chromium ions used to 50 mL solution at 25 °C, a contact time of 5 h, pH 2.0, and agitation rate (200 rpm). The pollutants of toxic metal less than 5% recovered used to basic media adsorbent and more than 94% acidic media desorption produce rapidly. A calibrated pH 2.0–4.0 after desorption with acid medium and resolve of the reusability

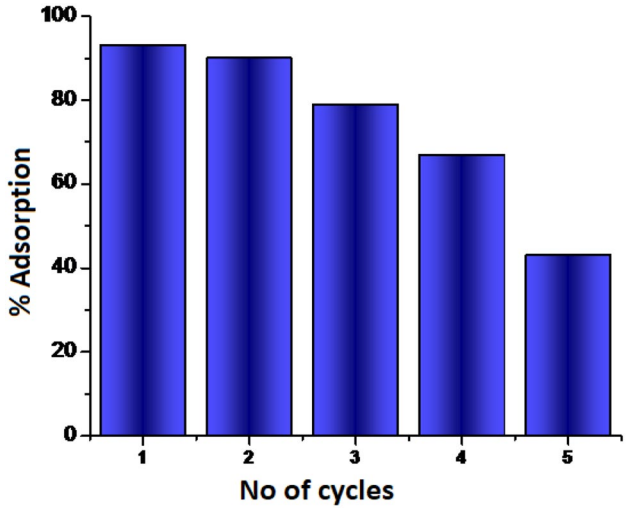

Fig. 10 Reusability of Fe_3O_4@PANI/IA magnetic nanocomposite

of sorbents of five times for desorption cycles was repetitive successively. These categories of the reusable study utilized for the elimination of various metal ion, heavy metal, and hazardous dye. Hence this kind of recycle method used for different industrial, environmental and chemical applications.

5 Conclusions

In this work, a simple steps and *in-situ* polymerization method for the preparation of Fe_3O_4@PANI/IA nanocomposite has been developed. The nanocomposite has a surface morphology and the shape of particle was studied by SEM and TEM techniques. The structure, elemental analysis, thermal and magnetic properties, and of the nanocomposites were investigated by FT-IR, EDS, TGA/DTA, and VSM. The maximum Cr (VI) ions removal percentage (92.2%) were studied by the adsorption process. The well supported experimental results data achieved from Langmuir and Freundlich adsorption isotherm model at different parameters. A new as-fabricated nanocomposite from PANI (conducting polymer) and IA (natural) one with iron nanoparticles can be considered eco-friendly adsorption that is characterized by its comfort of fabrication as well as its magnetic properties. Present research proved that Fe_3O_4@PANI/IA nanocomposites were reliable low cost and efficient adsorbent. Believing today's economic features of wastewater treatment and reducing water pollution, this adsorbent materials composite using capable and consistent sorbent for effective removal of chromium (VI) ion from wastewater.

References

1. J.G.S. Mala, D. Sujatha, C. Rose, Microbiol. Res. **170**, 235–241 (2015)
2. T. Karthikeyan, S. Rajgopal, L.R. Miranda, J. Hazard. Mater. **124**, 192–199 (2005)
3. S. Hokkanen, A. Bhatnagar, M. Sillanpaa, Water Res. **91**, 156–173 (2016)
4. S. Laurent, D. Forge, M. Port, A. Roch, C. Robic, L. VanderElst, R.N. Muller, Chem. Rev. **110**, 2574–2574 (2010)
5. S. Singh, K. Vishwakarma, S. Singh, S. Sharma, N.K. Dubey, V.K. Singh, S. Liu, D.K. Tripathi, D.K. Chauhan, Plant Gene. **11**, 265–272 (2017)
6. H. Shirakawa, E.J. Louis, A.G. MacDiarmid, J. Chem. Soc. Chem. Commun. **16**, 578–580 (1977)
7. P. Jain, S. Varshney, S. Srivastava, Appl. Water Sci. **7**, 1827–1839 (2017)
8. R. Zhang, H. Ma, B. Wang, Ind. Eng. Chem. Res. **49**, 9998–10004 (2010)
9. J. Zhang, J. Han, M. Wang, J. Mater. Chem. A. **5**, 4058–4066 (2017)
10. M. Mehdi Sadeghi, A. Shokuhi Rad, M. Ardjmand, A. Mirabi, Synth. Metals. **245**, 1–9 (2018)
11. K. Nitesh, K. Abhishek, V.K. Jain, S. Nagpal, Sep. Sci. Technol. **26**, 1–13 (2019)
12. S.J. Velickovic, E.S. Dzunuzovic, P.C. Griffiths, J. Appl. Polym. Sci. **26**, 3275–3282 (2008)
13. H. Zeghioud, S. Lamouri, Z. Safidine, M. Belbachir, J. Serb. Chem. Soc. **80**, 917–931 (2015)
14. M. Sakthivel, D.S. Franklin, S. Sudarsan, G. Chitra, T.P. Sridharan, S. Guhanathan, SN Appl. Sci. **1**, 146 (2019)
15. B. Eftekhari-Sis, A. Akbari, P. Yekan Motlagh, Z. Bahrami, N. Arsalani, J. Inorg. Organomet. **28**, 1728–1738 (2018)
16. C. Della Pina, M. Rossi, A. Maria Ferretti, A. Ponti, M. LoFaro, E. Falletta, Synth. Metals. **162**, 2250–2258 (2012)
17. S. Wang, H. Bao, P. Yang, G. Chen, Anal. Chim. Acta. **612**, 182–189 (2008)
18. A. Singh, A. Singh, S. Singh, P. Tandon, B.C. Yadav, R.R. Yadav, J. Alloy. Compd. **618**, 475–483 (2015)
19. M.R. Patil, S.D. Khairnar, S. Shrivastava, Appl. Nanosci. **6**, 495–502 (2016)
20. A. Singh, S. Singh, B.D. Joshi, A. Shukla, B.C. Yadav, P. Tandon, Mat. Sci. Semicon. Proc. **27**, 934–949 (2014)
21. A. Hsini, A. Essekri, N. Aarab, M. Laabd, A. Ait Addi, R. Lakhmiri, A. Albourine, Environ. Sci. Pollut. **24**, 10604–10620 (2020)
22. M.M. Ayad, W.A. Amer, M.G. Kotp, I.M. Minisy, A.F. Rehab, D. Kopecky, P. Fitl, RSC. Adv. **7**, 18553–18560 (2017)
23. B. Mu, J. Tang, L. Zhang, A. Wang, Sci. Rep. **7**, 5347 (2017)
24. S. Singh, A. Singh, B.C. Yadav, P. Tandon, Mat. Sci. Semicon. Proc. **23**, 122–135 (2014)
25. A. Olad, F. Farshi Azhar, M. Shargh, S. Jharfi, Poly. Eng. Sci. **54**, 1595–1607 (2014)
26. V. Bhusari, R. Dahake, S. Rayalu, A. Bansiwal, Adv. Nanopart. **5**, 67 (2016)
27. R. Ansari, Acta Chim. Slov. **53**, 88–94 (2006)
28. S. Agrawal, N.B. Singh, Desalin. Water. Treat. **52**, 1–10 (2015)
29. M.V. Kulkarni, A. Kasi Viswanath, R. Marimuthu, T. Seth, Poly. Eng. Sci. **44**, 1676–1681 (2004)
30. Y. Wang, H. Zheng, L. Jia, H. Li, T. Li, K. Chen, Y. Gu, J. Ding, J. Macromol. Sci. A. **51**, 619–624 (2014)
31. T. Yin, H. Zhang, G. Yang, L. Wang, Synth. Metals. **252**, 8–14 (2019)
32. M.M. Ayad, W.A. Amer, M. Whdan, J. Appl. Polym. Sci. **125**, 2695–2700 (2012)
33. G. Azizian, N. Riyahi Alam, S. Haghgoo, H. Reza Moghimi, R. Zohdiaghdam, B. Rafiei, E. Gorji, Nanoscale Res. Lett. **7**, 549 (2012)
34. A.C.V. De Araujo, R.J. De Oliveira, S. Alves Junior, A.R. Rodrigues, F.L.A. Achado, F.A.O. Cabral, W.M. De Azevedo, Synth. Metals. **160**, 685–690 (2010)
35. Y. Zhang, Q. Li, L. Sun, Y. Zhai, Environ. Eng. **137**, 1158–1164 (2011)
36. M. Bhaumik, A. Maity, V.V. Srinivasu, M.S. Onyango, J. Hazard. mater. **190**, 381–390 (2011)
37. Y. Wang, B. Zou, T. Gao, X. Wu, S. Lou, S. Zhou, J. Mater. Chem. **22**, 9034–9040 (2012)
38 X. Han, L. Gai, H. Jiang, L. Liu, H. Zhao, W. Zhang, Synth. Met. **171**, 1–6 (2013)
39. J. Chen, X. Hong, Y. Zhao, Y. Xia, D. Li, Q. Zhang, J. Mater. Sci. **48**, 7708–7717 (2013)
40. S. Agrawal, N.B. Singh, Desalin. Water. Treat. **57**, 17757–17766 (2015)
41. D.K.L. Harijan, V. Chandra, J. Appl. Polym. Sci. **133**, 44002–44007 (2016)
42. N. Ilankoon, Int. J. Eng. Res. Appl. **4**, 55–63 (2014)
43. A.G. Yavuz, E. Atalay, A. Uygun, F. Gode, E. Aslan, Desalination **279**, 325–331 (2014)
44. A. Olad, M. Bastanian, H.B. Khosh Hagh, J. Inorg. Organomet. **29**, 1916–1926 (2019)
45. M.A. Gabal, A.A. Al-Juaid, S. El-Rashed, M.A. Hussein, Y.M. Al Angari, A.J. Saeed, Inorg. Organomet. **29**, 2197–2213 (2019)